

1 Through The Back Door: Expiratory Accumulation Of SARS-Cov-2 In The 2 Olfactory Mucosa As Mechanism For CNS Penetration

3

4 Carlotta Pipolo¹, Antonio Mario Bulfamante¹, Andrea Schillaci², Jacopo Banchetti², Luca Castellani¹,
5 Alberto Maria Saibene¹, Giovanni Felisati¹ * & Maurizio Quadrio² *

6

7 *These authors are both last co-authors

8

9 ¹ Unit of Otolaryngology, ASST Santi Paolo e Carlo, Department of Health Sciences, Università degli
10 Studi di Milano, Milan, Italy

11 ² Dept. of Aerospace Science and Technologies, Politecnico di Milano, Italy

12

13

14

15

16

17

18

19

20 **Corresponding author**

21 Antonio Mario Bulfamante, MD

22 Università degli Studi di Milano

23 Otolaryngology Department

24 San Paolo Hospital

25 Via A. di Rudinì, 8

26 20142 Milan – Italy

27 Phone: +39 02 8184 4249 Fax: +39 02 5032 3166 Mail: antonio.bulfamante@unimi.it

28

29

30

31 **Keywords**

32 Computational Fluid Dynamics, SARS-Cov-2, Olfactory Mucosa, Nose

33

34

35

36

NOTE: This preprint reports new research that has not been certified by peer review and should not be used to guide clinical practice.

37 **Abstract**

38 **Introduction**

39 SARS-CoV-2 is a respiratory virus supposed to enter the organism through aerosol or fomite trans-
40 mission to the nose, eyes and oropharynx. It is responsible for various clinical symptoms, including
41 hyposmia and other neurological ones. Current literature suggests the olfactory mucosa as a port of
42 entry to the CNS, but how the virus reaches the olfactory groove is still unknown. Because the first
43 neurological symptoms of invasion (hyposmia) do not correspond to first signs of infection, the hy-
44 pothesis of direct contact through airborne droplets during primary infection and therefore during
45 inspiration is not plausible. The aim of this study is to evaluate if a secondary spread to the olfactory
46 groove in a retrograde manner during expiration could be more probable.

47 **Methods**

48 Four three-dimensional virtual models were obtained from real CT scans and used to simulate ex-
49 piratory droplets. The volume mesh consists of 25 million of cells, the simulated condition is a steady
50 expiration, driving a flow rate of 270 ml/s, for a duration of 0.6 seconds. Droplet diameter is of 5
51 μm .

52 **Results**

53 The analysis of the simulations shows the virus to have a high probability to be deployed in the
54 rhinopharynx, on the tail of medium and upper turbinates. The possibility for droplets to access the
55 olfactory mucosa during the expiratory phase is lower than other nasal areas, but consistent.

56

57 **Discussion**

58 The data obtained from these simulations demonstrates that virus can be deployed in the olfactory
59 groove during expiration. Even if the total amount in a single act is very low, it must be considered
60 that it is repeated tens of thousands of times a day, and the source of contamination continuously
61 acts on a timescale of several days. The present results also imply CNS penetration of SARS-CoV-2
62 through olfactory mucosa might be considered a complication and, consequently, prevention strat-
63 egies should be considered in diseased patients.

64

65 **Abbreviations**

66 SARS-CoV-2: severe acute respiratory syndrome coronavirus 2; CT: computed tomography; CNS:
67 Central nervous system; LES: Large eddy simulation; CFD: Computational fluid dynamics; ACE-2: An-
68 giotensin converting enzyme; COVID-19: Coronavirus disease 2019

69 **Introduction**

70

71 SARS-CoV-2 is a respiratory virus, still widely spreading throughout the globe, that is thought to
72 enter the organism through aerosol or fomite transmission to the nose, eyes and oropharynx (1,2).
73 Presentation ranges from respiratory symptoms such as cough and fever to neurological symptoms
74 such as headache, dizziness and hyposmia, showing different target organs of the virus (3,4). Current
75 literature has recently started to study access points into the CNS and the anatomical proximity
76 between neurons, nerve fibers and the mucosa within the olfactory groove (5); the reported clinical-
77 neurological signs related to alteration in smell suggest that SARS-CoV-2 exploits this neuro-mucosal
78 interface as port of entry. Even though early reports (6) are indeed supporting this hypothesis
79 through autopsy sampling, no literature exists as to how the SARS-CoV-2 reaches the mucosa at the
80 level of the olfactory cleft, and whether the olfactory mucosa involvement is a direct consequence
81 of viral particle deposition or due to a secondary viral invasion of these tissues during the course of
82 the infection.

83 From other respiratory viruses we know that aerosols, which are responsible for the transmission
84 of airborne microorganisms, consist of small droplet nuclei (1–5 μ m) or droplets (>5 μ m) (7); these
85 have specific characteristics regarding their distribution inside the nose and respiratory tract.
86 Considering that the first neurological symptoms of invasion (hyposmia) do not correspond to first
87 signs of presentation of infection, the hypothesis of direct contact through airborne at the stage of
88 primary infection and therefore during inspiration is not plausible.

89 The second hypothesis of a secondary spread to the olfactory groove in a retrograde manner during
90 for example expiration in an already challenged organism seems to be more likely. This would make
91 CNS penetration a complication secondary to e.g. pulmonary infection, thus opening the field to so
92 far unconsidered preventative measures.

93 Our group has therefore used computational fluid dynamics to study distribution of airflow and
94 deposition of supposed infectious sub-micron droplets during breathing, to better understand the
95 possible routes of infection and penetration inside the nasal cavities and the olfactory mucosa.

96

97 **Materials and Methods**

98 This study was granted exemption from the Institutional Review Board of the San Paolo Hospital,
99 Milano, Italy, due to its retrospective nature and is based on a set of CFD simulations of breathing,

100 where only expiration is considered. The Large Eddy Simulation (LES) technique on CT scan
101 reconstructions of nasal anatomies is used. LES is a high-cost and high-fidelity CFD approach, which
102 allows fine control over the modelling error in dealing with complex and possibly turbulent flows.
103 LES numerical simulations were performed starting from a set of four CT scans, whose sinonasal
104 anatomy was defined by consensus by all authors as devoid of any appreciable anatomic anomaly
105 (i.e. a straight septum, normotrophic turbinates with orthodox bending, symmetrical distribution of
106 anatomical features among the two sinonasal emi-systems).
107 CT scans have a 512×512 matrix with a $0.49 \text{ mm} \times 0.49 \text{ mm}$ spatial resolution in the sagittal-coronal
108 plane and a 0.625 mm gap between consecutive axial slices, with 250-350 native images for each
109 case. More details on CT images processing, choice of the threshold value and 3D reconstruction,
110 carried out via the software 3D Slicer (9), have been already reported in the literature documenting
111 the entire procedure (10–14). The CFD simulations were carried out with the finite-volumes
112 OpenFOAM software package (15).
113 The CFD analysis of each of the four cases (patients from P1 to P4) was conducted on finely
114 discretized volume mesh consisting of 25 million of cells, yielding extreme accuracy. The simulated
115 condition is a steady expiration driving a flow rate of 270 ml/s , which corresponds to low to medium
116 intensity breathing (16), for a duration of 0.6 seconds. A large number of droplets with diameter of
117 $5 \mu\text{m}$, in accordance with the expected droplet size described above (7), was placed at the lower
118 boundary of the computational domain and allowed to enter as time progresses. Droplets are
119 transported by the airflow, and most of them are exhaled after travelling through the nasal
120 chamber, becoming responsible for the potential airborne contagion. Because of their inertia,
121 however, a fraction of the droplets deposits on the mucosal lining of the nose. The simulations
122 identify the deposited droplets, and therefore provide a representation of the deposition pattern,
123 highlighting areas of preferential deposition during expiration. Particular attention is given to the
124 particles that reach the olfactory slit, qualitatively sketched in figure 1. This study provides
125 information on the preferential site of adhesion of expiratory droplets to the olfactory mucosa and
126 computes the spatially varying degree of probability for a droplet to deposit in a specific location
127 instead of being convected to the external ambient.

128

129 **Results**

130 The simulations portrait the preferential sites of droplet deposition on the nasal mucosa during
131 expiration. It is clearly visible in Figure 2, 3 and 4 that, although virus deposition is prevalent in the

132 nasal vestibule and rhinopharynx. some droplets indeed do deposit in the area corresponding to the
133 olfactory mucosa. Moreover, as expected, interindividual differences are visible. Droplets have been
134 emphasized with a red dot.

135 The analysis of sagittal sections (fig. 2, where only the left nasal fossa is shown for clarity) shows the
136 virus to have a high probability to be deployed in the rhinopharynx, on the tail of medium and upper
137 turbinates. The possibility for droplets to access the olfactory mucosa during the expiratory phase
138 is of primary interest. The evaluation of axial projections (Fig. 3) confirms a high concentration of
139 particles in the posterior segments in addition to a better visualisation of particle distribution
140 between medial and lateral compartments. Although heterogeneously, it can be observed how the
141 particles, and consequently the virus, are more likely to settle in the medial quadrants of the nasal
142 cavities than in lateral ones. During the expiratory phase, the particles have a significant probability
143 to impact and adhere to the mucosa of the ethmoidal rostrum. Finally, the analysis of coronal
144 projections (Fig. 4) confirms previous observations, although it demonstrates a better visualisation
145 of the septal rostrum region and of both portions of the rhinopharynx. Coronal projections confirm
146 that indeed some particles reach of the olfactory slit.

147

148 **Discussion**

149 Regardless of the mechanism for viral transmission (direct respiratory, aerosol or fomite), first
150 access to the nose must happen through inspiration. Once the virus has gained entry to the sinonasal
151 cavities, however, many different potential mechanisms concur to further diffusion, among which
152 transport, local replication, and invasion of proximal structures. The ability of SARS-CoV-2 to bind
153 the ACE-2 receptor, enter the respiratory epithelium cells and thereby initiate its replication has
154 been thoroughly demonstrated (17,18).

155 Respiratory droplets containing viral particles are unable to massively reach the olfactory cleft,
156 which should not be therefore considered as a primary target for COVID-19 infection. The droplet
157 ability to deposit on the olfactory cleft is a direct function of the particle size, given that the olfactory
158 cleft is anatomically developed to receive smaller particles such as odorants, while droplets carrying
159 the viral load can be larger (8). Such an ineffective viral deposition on to the olfactory mucosa,
160 coupled with the known defensive mechanisms employed by the olfactory mucosa to protect from
161 environmental noxae (17,19), make the direct infection of the olfactory cleft by SARS-CoV-2 at the
162 time of primary entry into the organism unlikely at best. On the other hand, cumulative exposure of
163 the olfactory cleft to expiratory droplets from the lower respiratory tract in an already diseased

164 organism may be more likely. In fact, the viral load in the lung is much higher than a one-time aerosol
165 reaching the nose, the act of expiration is repeated tens of thousands of times a day, and the source
166 of contamination continuously acts on a timescale of several days. This route to the olfactory cleft
167 and maybe to CNS may also explain the time lag between first symptoms and first neurological
168 impairments such as hyposmia (20,21).

169

170 The present results also imply that CNS penetration of SARS-CoV-2 through olfactory mucosa might
171 be a complication of an already present infection of the lower respiratory tract. Hence, prevention
172 of the olfactory mucosa penetration by the virus should be considered in diseased patients. High
173 volumes nasal washes, usually performed with saline, can be used to reduce the adherence of viral
174 parts emitted from the lower respiratory tract towards the nasal cavities, thus weakening the virus
175 ability to spread to the olfactory mucosa. Indeed, other authors have advocated the use of nasal
176 lavages in SARS-CoV-2 infection as a preventive measure (22), and prior studies on viral upper
177 respiratory tract infections with hypertonic saline showed reduced viral shedding and patients
178 infectivity (23) in the already diseased. Prior studies on viral upper respiratory tract infections with
179 hypertonic saline showed decreased viral shedding and reduced patients infectivity (23) in in the
180 already diseased. Others propose other types of medications: in (24) inhalation of acetic acid is
181 suggested to be effective in shortening duration of symptoms. The present study -- besides
182 suggesting the olfactory region as a target for inhibition of the secondary viral infection which
183 endangers the CNS -- provides further support for the effectiveness of such preventive measures,
184 since a diffuse droplet deposition takes place in the nasal fossae, that can be easily reached by
185 washing or by other nasal medications.

186 Further studies are thus required to focus on nasal washes not only as a preventive measure to
187 infection but also as a means to inhibit the secondary spreading of the virus to the olfactory mucosa
188 and therefore to the CNS for COVID-19 patients. These studies should clinically quantify the ability
189 of nasal washes, i.e. a simple and non-invasive treatment, to halt the progression of the disease by
190 containing its complications involving the CNS.

191

192 **Competing interests**

193 The authors have declared that no competing interest exists

194 **References**

- 195
196
197 1. van Doremalen N, Bushmaker T, Morris DH, Holbrook MG, Gamble A, Williamson BN, et al. Aerosol and
198 Surface Stability of SARS-CoV-2 as Compared with SARS-CoV-1. *New England Journal of Medicine*.
199 2020 Apr 16;382(16):1564–7.
- 200 2. Kwok YLA, Gralton J, McLaws M-L. Face touching: a frequent habit that has implications for hand
201 hygiene. *Am J Infect Control*. 2015 Feb;43(2):112–4.
- 202 3. Cui C, Yao Q, Zhang D, Zhao Y, Zhang K, Nisenbaum E, et al. Approaching Otolaryngology Patients
203 During the COVID-19 Pandemic. *Otolaryngol Head Neck Surg*. 2020 Jul 1;163(1):121–31.
- 204 4. Tong JY, Wong A, Zhu D, Fastenberg JH, Tham T. The Prevalence of Olfactory and Gustatory
205 Dysfunction in COVID-19 Patients: A Systematic Review and Meta-analysis. *Otolaryngol Head Neck*
206 *Surg*. 2020;163(1):3–11.
- 207 5. Doty RL. The olfactory vector hypothesis of neurodegenerative disease: is it viable? *Ann Neurol*. 2008
208 Jan;63(1):7–15.
- 209 6. Bulfamante G, Chiumello D, Canevini MP, Priori A, Mazzanti M, Centanni S, et al. First ultrastructural
210 autoptic findings of SARS -Cov-2 in olfactory pathways and brainstem. *Minerva Anestesiol*.
211 2020;86(6):678–9.
- 212 7. Zemouri C, de Soet H, Crielaard W, Laheij A. A scoping review on bio-aerosols in healthcare and the
213 dental environment. *PLoS One*. 2017;12(5):e0178007.
- 214 8. Zhao K, Scherer PW, Hajiloo SA, Dalton P. Effect of anatomy on human nasal air flow and odorant
215 transport patterns: implications for olfaction. *Chem Senses*. 2004 Jun;29(5):365–79.
- 216 9. 3D Slicer: A Platform for Subject-Specific Image Analysis, Visualization, and Clinical Support |
217 SpringerLink [Internet]. [cited 2020 Nov 3]. Available from: [https://link.springer.com/chapter/10.1007/978-](https://link.springer.com/chapter/10.1007/978-1-4614-7657-3_19)
218 [1-4614-7657-3_19](https://link.springer.com/chapter/10.1007/978-1-4614-7657-3_19)
- 219 10. Saibene AM, Felisati G, Pipolo C, Bulfamante AM, Quadrio M, Covello V. Partial Preservation of the
220 Inferior Turbinate in Endoscopic Medial Maxillectomy: A Computational Fluid Dynamics Study. *Am J*
221 *Rhinol Allergy*. 2020 May;34(3):409–16.
- 222 11. Buijs EFM, Covello V, Pipolo C, Saibene AM, Felisati G, Quadrio M. Thermal water delivery in the nose:
223 experimental results describing droplet deposition through computational fluid dynamics. *Acta*
224 *Otorhinolaryngol Ital*. 2019 Dec;39(6):396–403.
- 225 12. Covello V, Pipolo C, Saibene A, Felisati G, Quadrio M. Numerical simulation of thermal water delivery in
226 the human nasal cavity. *Comput Biol Med*. 2018 01;100:62–73.
- 227 13. Quadrio M, Pipolo C, Corti S, Lenzi R, Messina F, Pesci C, et al. Review of computational fluid dynamics
228 in the assessment of nasal air flow and analysis of its limitations. *Eur Arch Otorhinolaryngol*. 2014
229 Sep;271(9):2349–54.
- 230 14. Quadrio M, Pipolo C, Corti S, Messina F, Pesci C, Saibene AM, et al. Effects of CT resolution and
231 radiodensity threshold on the CFD evaluation of nasal airflow. *Med Biol Eng Comput*. 2016 Mar;54(2–
232 3):411–9.
- 233 15. Weller HG, Tabor G, Jasak H, Fureby C. A tensorial approach to computational continuum mechanics
234 using object-oriented techniques. *Computers in Physics*. 1998 Nov 1;12(6):620–31.
- 235 16. Calmet H, Gambaruto AM, Bates AJ, Vázquez M, Houzeaux G, Doorly DJ. Large-scale CFD simulations
236 of the transitional and turbulent regime for the large human airways during rapid inhalation. *Computers*
237 *in Biology and Medicine*. 2016 Feb 1;69:166–80.

- 238 17. Hui KPY, Cheung M-C, Perera RAPM, Ng K-C, Bui CHT, Ho JCW, et al. Tropism, replication
239 competence, and innate immune responses of the coronavirus SARS-CoV-2 in human respiratory tract
240 and conjunctiva: an analysis in ex-vivo and in-vitro cultures. *The Lancet Respiratory Medicine*. 2020 Jul
241 1;8(7):687–95.
- 242 18. Hoffmann M, Kleine-Weber H, Schroeder S, Krüger N, Herrler T, Erichsen S, et al. SARS-CoV-2 Cell
243 Entry Depends on ACE2 and TMPRSS2 and Is Blocked by a Clinically Proven Protease Inhibitor. *Cell*.
244 2020 Apr;181(2):271-280.e8.
- 245 19. Herbert RP, Harris J, Chong KP, Chapman J, West AK, Chuah MI. Cytokines and olfactory bulb
246 microglia in response to bacterial challenge in the compromised primary olfactory pathway. *J*
247 *Neuroinflammation*. 2012 May 29;9:109.
- 248 20. Ahmad I, Rathore FA. Neurological manifestations and complications of COVID-19: A literature review. *J*
249 *Clin Neurosci*. 2020 Jul;77:8–12.
- 250 21. Niazkar HR, Zibae B, Nasimi A, Bahri N. The neurological manifestations of COVID-19: a review
251 article. *Neurol Sci*. 2020 Jul;41(7):1667–71.
- 252 22. Singh S, Sharma N, Singh U, Singh T, Mangal DK, Singh V. Nasopharyngeal wash in preventing and
253 treating upper respiratory tract infections: Could it prevent COVID-19? *Lung India*. 2020 Jun;37(3):246–
254 51.
- 255 23. Ramalingam S, Graham C, Dove J, Morrice L, Sheikh A. A pilot, open labelled, randomised controlled
256 trial of hypertonic saline nasal irrigation and gargling for the common cold. *Sci Rep*. 2019 31;9(1):1015.
- 257 24. Pianta L, Vinciguerra A, Bertazzoni G, Morello R, Mangiatordi F, Lund VJ, et al. Acetic acid disinfection
258 as a potential adjunctive therapy for non-severe COVID-19. *Eur Arch Otorhinolaryngol*. 2020
259 Oct;277(10):2921–4.

260
261
262
263
264
265
266
267
268
269
270
271
272
273
274
275
276
277
278
279
280
281
282
283
284
285
286
287
288
289
290
291
292
293
294
295
296
297
298
299
300
301
302
303
304
305
306
307
308
309
310
311
312
313
314
315
316
317
318
319
320
321
322
323
324
325
326
327
328

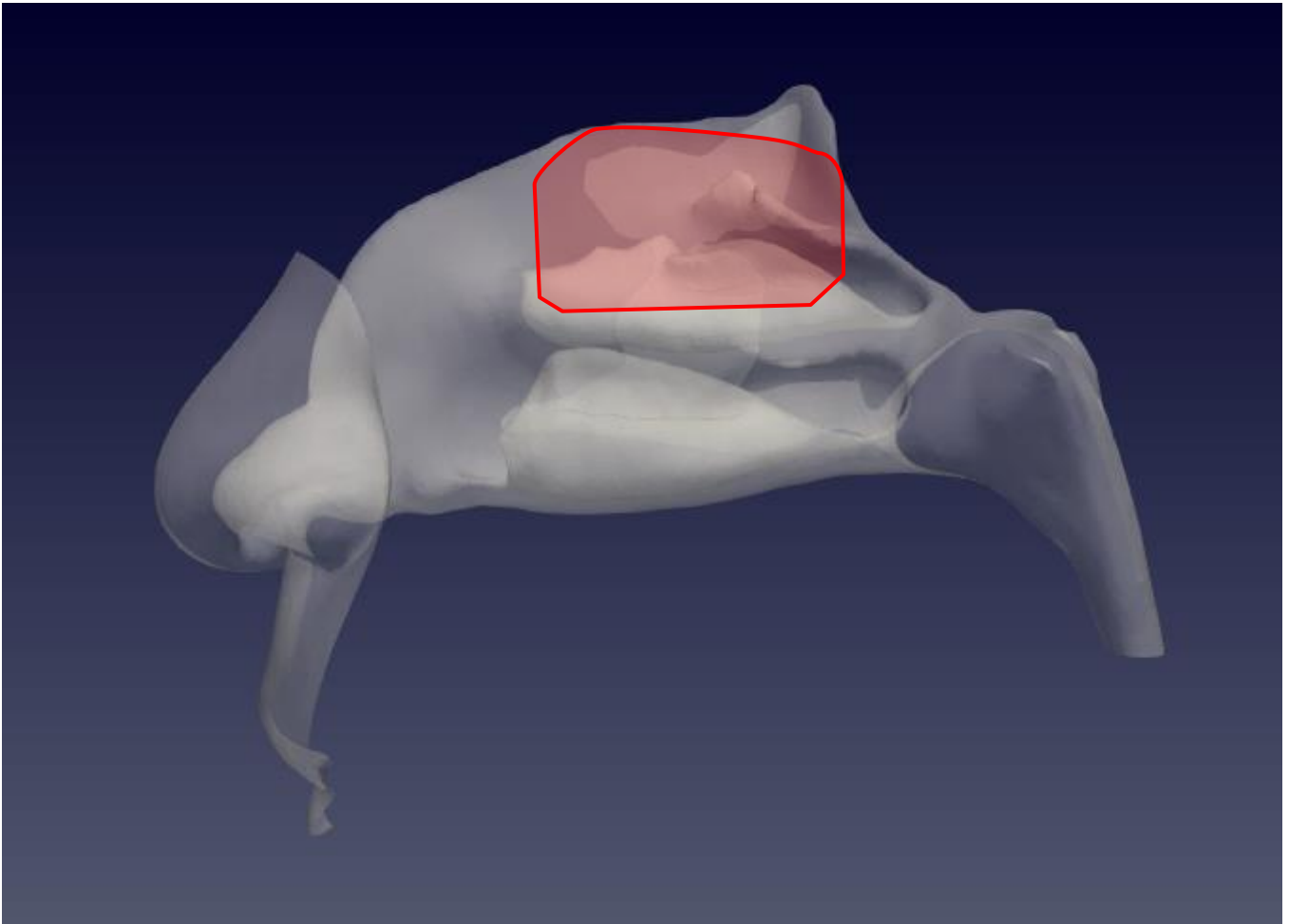
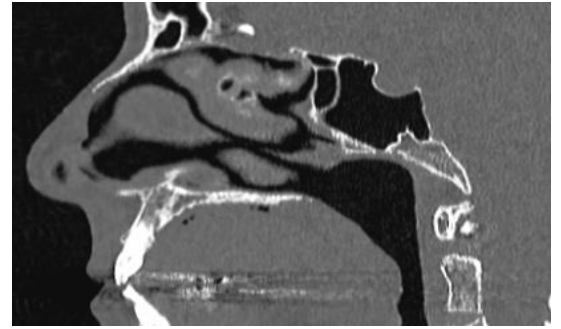
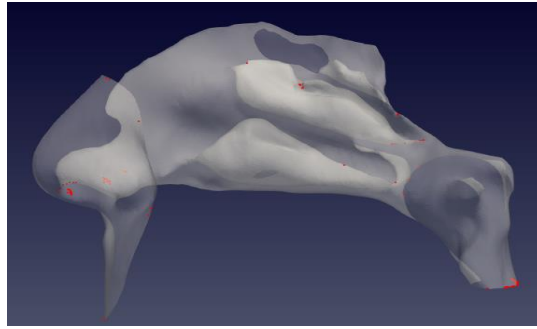


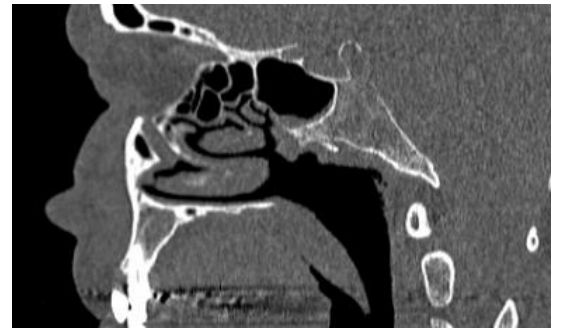
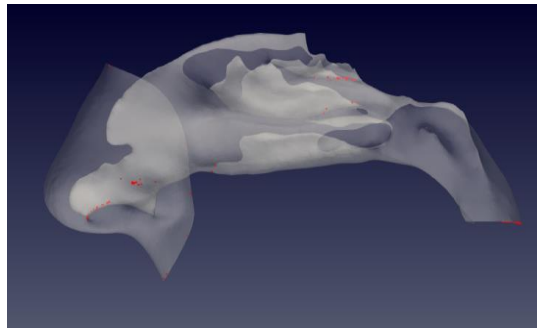
Figure 1 Sagittal view of the left nostril. The olfactory slit is highlighted in red.

329
330
331
332
333
334
335
336
337
338
339
340
341
342
343
344
345
346
347
348
349
350
351
352
353
354
355
356
357
358
359
360
361
362
363
364
365
366
367
368
369
370
371
372
373
374
375
376
377
378
379
380
381
382
383
384
385
386
387
388
389
390
391
392
393
394
395
396
397

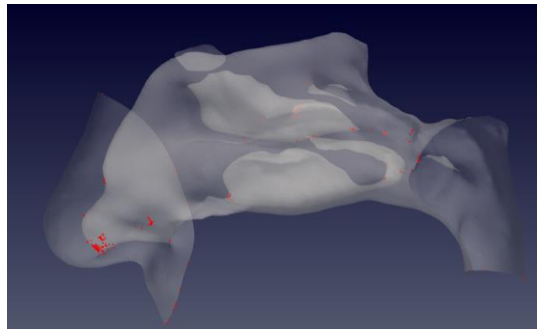
P1



P2



P3



P4

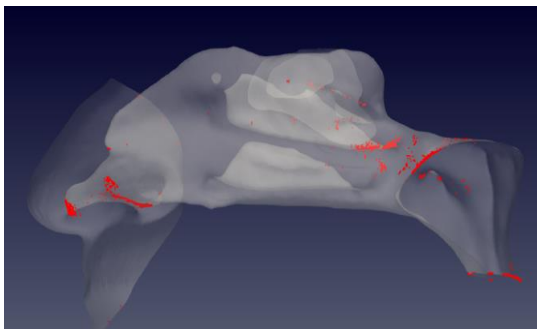


Figure 2 Distribution of droplet deposition during expiration, in sagittal projection. 3D models of the nasal fossae (left column), obtained from the CT, which are shown in the right panel. Particle size is increased to improve clarity.

398
399
400
401
402
403
404
405
406
407
408
409
410
411
412
413
414
415
416
417
418
419
420
421
422
423
424
425
426
427
428
429
430
431
432
433
434
435
436
437
438
439
440
441
442
443
444
445
446
447
448
449
450
451
452
453
454
455
456
457
458
459
460
461
462
463
464
465
466

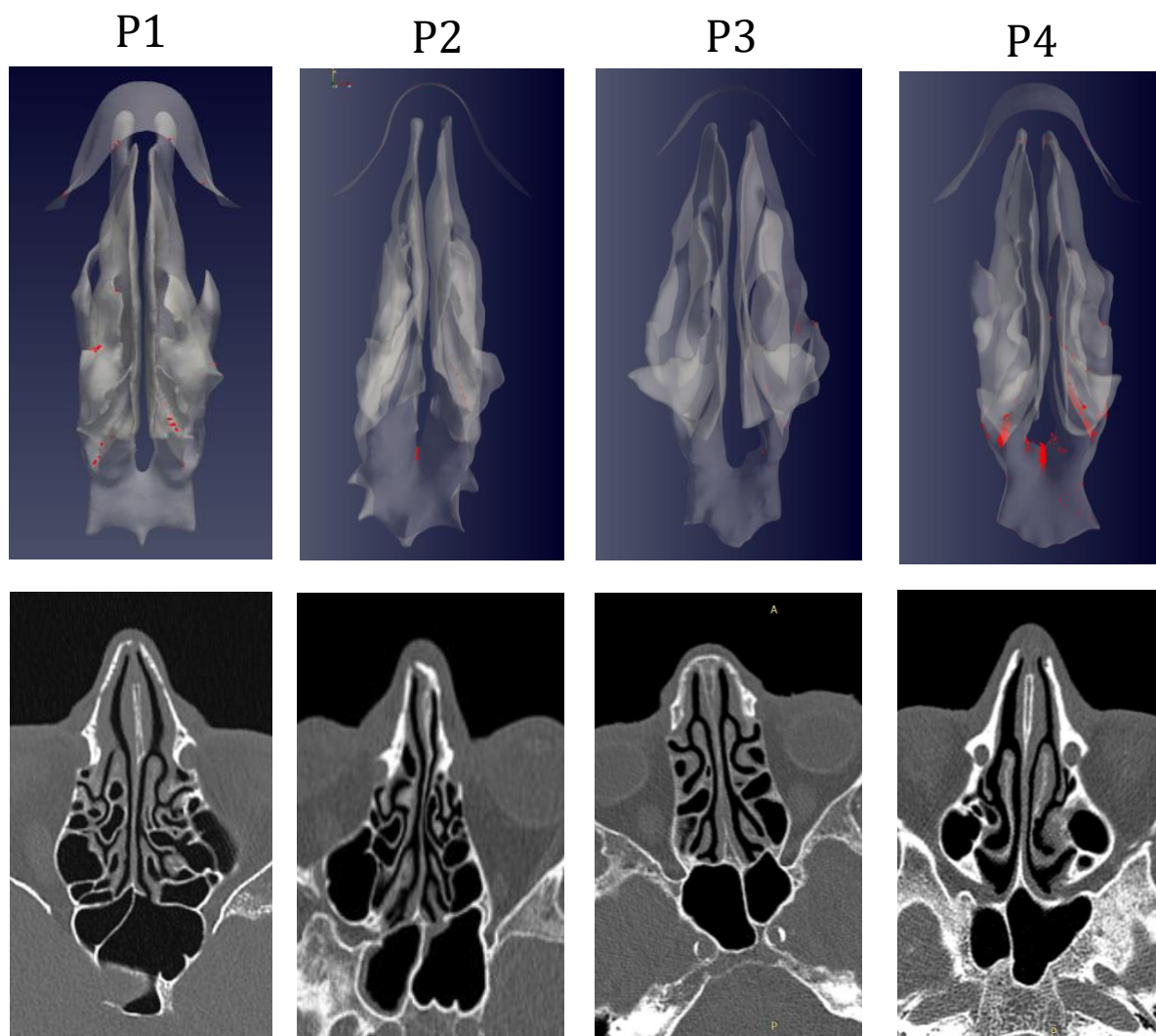


Figure 3: As in figure 1, but axial projection.

467
468
469

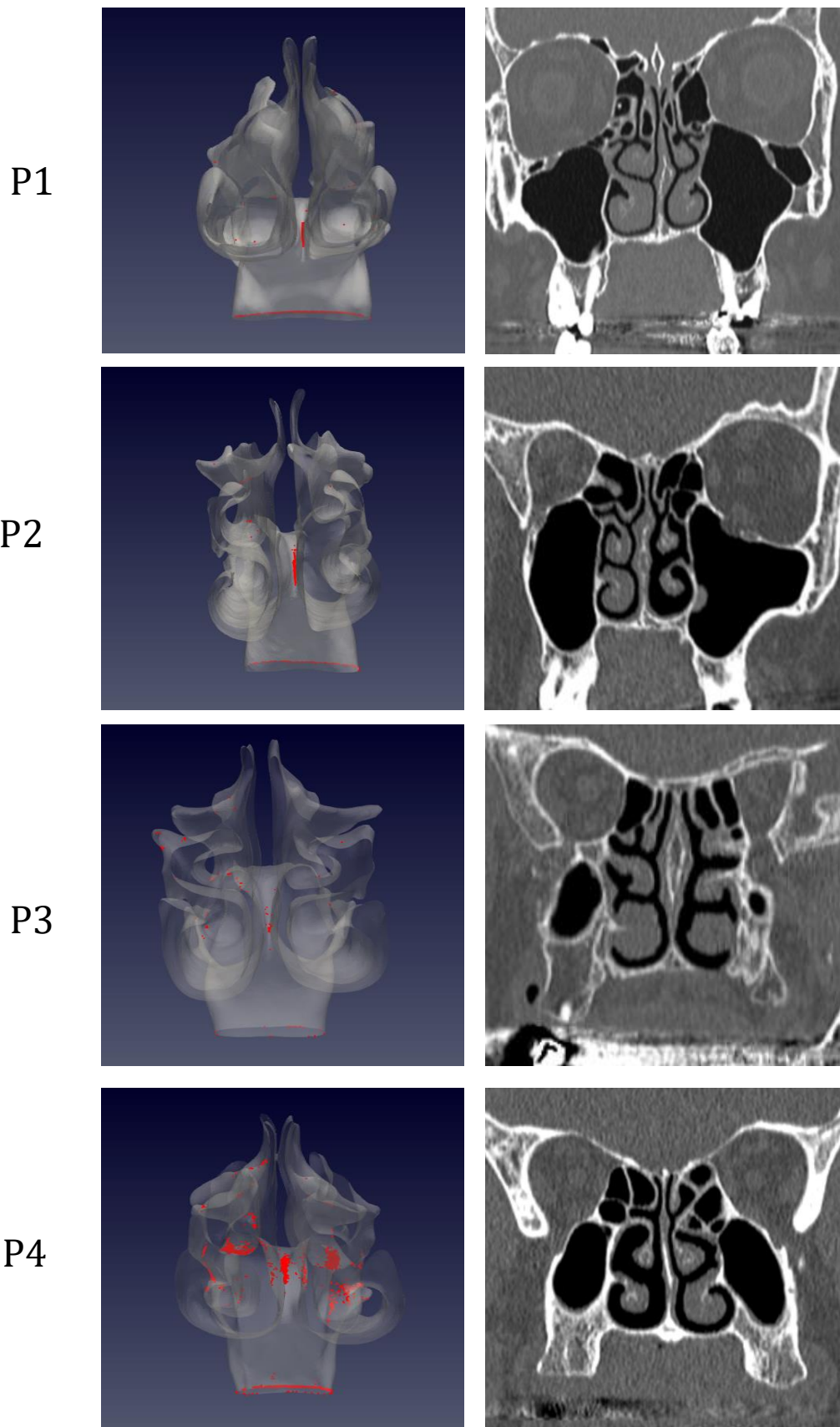


Figure 4: As in figure 1, but coronal projection.